cutaneous albinism) gene. Proc Natl Acad Sci USA 91: 12071–12075

Rosemblat S, Sviderskaya EV, Easty DJ, Wilson A, Kwon BS, Bennett DC, Orlow SJ (1998) Melanosomal defects in melanocytes from mice lacking expression of the pink-eyed dilution gene: correction by culture in the presence of excess tyrosine. Exp Cell Res 239: 344–352

Russell ES (1949) A quantitative histological study of the pigment found in the coat-color mutants of the house mouse. IV. The nature of the effects of genic substitution in five major allelic series. Genetics 34: 146–166

Seiji M, Shimao K, Birbeck MSC, Fitzpatrick TB (1963) Subcellular localization of melanin biosynthesis. Ann NY Acad Sci 100: 497–533

Sidman RL, Pearlstein R (1965) Pink-eyed dilution (p) gene in rodents: increased pigmentation in tissue culture. Dev Biol 12: 93–116

Silvers WK (1979) The Coat Colors of Mice. Springer-Verlag, Berlin

Slominski A, Jastreboff P, Pawelek J (1989) L-tyrosine stimulates induction of tyrosinase activity by MSH and reduces cooperative interactions between MSH receptors in hamster melanoma cells. Biosci Rep 9: 579–586

Staleva L, Manga P, Orlow SJ (2002) Pink-eyed dilution protein modulates arsenic sensitivity and intracellular glutathione metabolism. Mol Biol Cell 13: 4206–4220

Tamate HB, Hirobe T, Wakamatsu K, Ito S, Shibahara S, Ishikawa K (1989) Levels of tyrosinase and its mRNA in coat-color mutants of C57BL/10J congenic mice: effects of genic substitution at the agouti, brown, albino, dilute, and pink-eyed dilution loci. J Exp Zool 250: 304–311

Thody AJ, Ridley K, Penny RJ, Chalmers R, Fisher C, Shuster S (1983) MSH peptides are present in mammalian skin. Peptides 4: 813–816

Toyofuku K, Valencia JC, Kushimoto T, Costin G-E, Virador VM, Viera WD, Ferrans VJ, Hearing VJ (2002) The etiology of oculocutaneous albinism (OCA) type II: the pink protein modulates the processing and transport of tyrosinase. Pigment Cell Res 15: 217–224

Wakamatsu K, Hirobe T, Ito S (2007) High levels of melanin-related metabolites in plasma from pink-eyed dilution mice. Pigment Cell Res 20: 222–224

Yaar M, Grossman K, Eller M, Gilchrest BA (1991) Evidence for nerve growth factor-mediated paracrine effects in human epidermis. J Cell Biol 115: 821–828

Yada Y, Higuchi K, Imokawa G (1991) Effects of endothelins on signal transduction and proliferation in human melanocytes. J Biol Chem 266: 18352–18357

Yohn JJ, Morelli JG, Walchak SJ, Rundell KB, Norris DA, Zamora MR (1993) Cultured human keratinocytes synthesize and secrete endothelin-1. J Invest Dermatol 100: 23–26

Multiple Analysis of Respiratory Activity in the Identical Oocytes by Applying Scanning Electrochemical Microscopy

Masaki Yokoo[1], Takahiro Ito-Sasaki[2], Hitoshi Shiku[3], Tomokazu Matsue[3], Hiroyuki Abe[2*]

[1]Innovation of New Biomedical Engineering Center, Tohoku University, Sendai, Japan; [2]Graduate Program of Human Sensing and Functional Sensor Engineering, Graduate School of Science and Engineering, Yamagata University, Yonezawa, Japan; [3]Graduate School of Environmental Studies, Tohoku University, Sendai, Japan

*To whom correspondence should be addressed Fax: 81-238-26-3361; e-mail: abeh@yz.yamagata-u.ac.jp

Scanning electrochemical microscopy (SECM) is a technique in which the tip of a microelectrode is used to scan and monitor the local distribution of electro-active species near the sample surface. In this study, we have studies on the SECM technique, to establish the accurate method for measurement of respiratory activity of single pig oocytes. The oxygen consumption rates of pig oocytes cultured in modified TCM199 medium were evaluated by the SECM system. After the measuring, distribution of active mitochondria and ATP content was investigated in the identical oocytes. The oocytes were classified in three types (Type-I, Type-II or Type-III) according to the pattern of active mitochondria distribution. There was no difference in the oxygen consumption rate ($F \times 10^{14}$/mol s^{-1}) between Type-II and Type-III (0.59 and 0.60, respectively). However, the ATP content (pmol/oocyte) was significantly higher in Type-III (2.38) compared with that of Type-II (1.53). Meanwhile, the oxygen consumption rate and ATP content of Type-I were very low (0.02 and 0.06, respectively). These results suggest that the oxygen consumption rate and ATP content of oocytes was significantly affected by category of mitochondrial distribution. In the present study, we succeeded in the multiple analysis of respiratory activity in the identical oocytes. This novel system may be a valuable tool for accurately assessing the mitochondrial functions.

Key words: cell respiration; electrochemical miscroscopy; pig oocyte; culture

INTRODUCTION

Oxygen consumption is an indicator of the overall metabolic activity and quality of a single embryo. Oxygen consumption of mammalian embryos has been with various methods such as Cartesian diver [1], spectrophotometrics [2, 3], fluorescence [4, 5] and electrochemical techniques [6], To establish the evaluation method for embryo quality based on the oxygen consumption activity, we have been studied on the scanning electrochemical microscopy (SECM) technique [7]. SECM technique has been successfully applied to investigate various biological systems including DNA [8], enzyme [9], antigen-antibodies [10,11], tissue [12], and cell [13], because of its non-invasive nature to quantitatively characterize localized chemical reaction under physiological conditions. In the previous study, we applied SECM technique to measure the oxygen consumption of single bovine embryos [14]. The oxygen consumption of individual bovine embryos produced in vitro fertilization (IVF) systems has been determined non-invasively and quantitatively by this technique. Furthermore, we have found that

there was a close relationship between high oxygen consumption and developmental ability of bovine embryos [14-16]. The SECM procedures may be useful to assess the quality of embryos and contribute to improvements in reproductive technologies in mammals.

On the other hand, an accurate system to evaluate oocyte quality is lacking. The most convenient evaluation system for oocyte quality is based on oocyte morphology and status of oocyte-cumulus complexes (COCs). However, this evaluation method could be imprecise and subjective, since there is no clear correlation between oocyte quality and fertilization rates [17]. Oocyte quality could be one of the most important factor in determining successful fertilization and embryo development. Therefore, we attempt to establish an evaluation system for oocyte quality is based on the respiratory activity of oocytes. The aims of this study were: 1) to assess the oxygen consumption of single pig oocytes using SECM; 2) to examine the mitochondrial distribution and ATP content in the identical oocytes.

MATERIAL AND METHODS

Scanning electrochemical microscopy measuring system

In this study, oxygen consumption was measured by SECM procedure [16, 18]. This modified SECM system includes a measuring instrument on an inverted optical microscope stage, a potentiostat (Hokuto Denko Co., Tokyo, Japan), and a notebook computer as controller and analyzer (Fig. 1a-d).
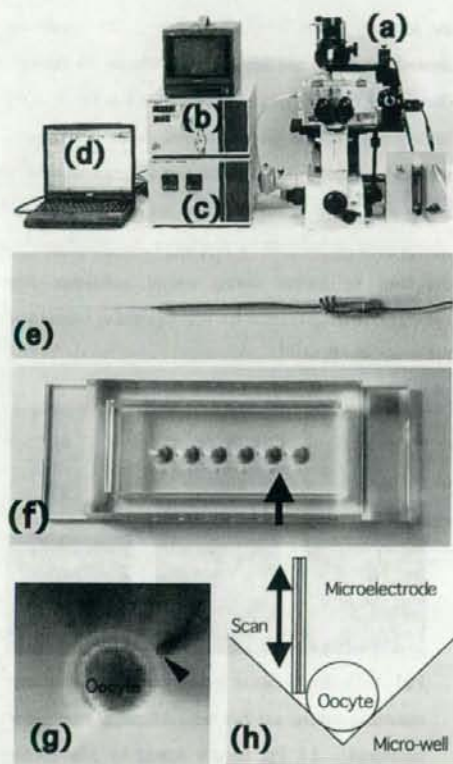

Fig. 1. A modified scanning electrochemical microscopy (SECM) system. SECM system includes a measuring instrument on the inverted optical microscope stage (a), potentiostat (b), controller (c), notebook computer (d), a microelectrode (e), and a plate (f) for measuring respiration activity of embryos. The plate has six cone-shaped microwells (arrow in f). Individual oocyte is transferred into a microwell filled with medium. The oocyte sinks down to the bottom of the well, remaining at the lowest point (g). Microelectrode (arrowhead in g) is scanned along the z-axis from the side point of oocyte (h).

Pt-microdisk electrodes sealed in a tapered soft-glass capillary were fabricated according to the method [19] (Fig. 1e). The tip potential was held at -0.6V versus Ag/AgCl with a potentiostat to monitor the local oxygen concentration in the solution. For the measurement of oxygen consumption, modified human tubal fluid (HTF) medium [20] was employed. Its composition only includes salt electrolyte, glucose, sodium pyruvate, sodium lactate, HEPES and gentamicin sulfate. Voltammetry of the Pt-microdisk electrode in modified HTF medium showed a steady-state oxygen reduction wave. No response from other electrochemically active species was observed near the oocyte surface. The tip scanning rate was 31.1 μm/s. The microelectrode with a Pt-disk radius less than 3 μm was selected so that the oxygen reduction current of the electrode was less than 1.0 nA. To easily handle many oocytes in a short time, a plate with cone-shaped microwells was used (Fig. 1f). The single pig oocyte was transferred into a cone-shaped microwell filled with modified HTF medium and oocyte fell to the bottom of the well and remained at the lowest point. The microelectrode was scanned according to the z-direction from side point of sample (so-called "side-scanning"; Fig. 1g, h). The motor driven XYZ-stage was located on the microscope stage for electrode tip scanning. The XYZ stage and potentiostat were controled by computer. The oxygen consumption rate of oocytes is calculated by newly designed software.

Oocyte collection and maturation culture

Pig cumulus-oocyte complexes (COCs) were obtained from ovarian follicles 2-5 mm in diameter. COCs classified as good quality by morphological evaluation were cultured in TCM199 medium containing 2.2 mg/ml sodium pyruvate, 10 mg/ml bovine serum albumin (BSA), 100 IU/ml penicillin, 100 μg/ml streptomycin, and 10% pig follicular fluid for *in vitro* maturation (IVM) in a humidified atmosphere of 5% CO_2 in air at 37.0°C for 48 h. After the cultures, cumulus cells were completely removed by the pipetting. The oxygen consumption of single denuded oocyte was measured by SECM systems. After the measurement, oocytes were prepared for histological (mitochondrial distribution) and biochemical (ATP content) experiments.

Staining of mitochondria

Oocytes were stained by MitoTracker Orange (Invitrogen;

Carlsbad, CA). This dye becomes fluorescent once it accumulates in the membrane lipids of mitochondria with membrane potential and is an important tool for evaluating the distribution of active mitochondria. MitoTracker Orange was used at a concentration of 350 nM in HPM199 medium (based on TCM199) supplemented 0.5% BSA for 30 min at 37.0°C. Oocytes were washed three times, mounted in a drop of HPM199 medium and examined using a confocal laser scanning microscope (FV-300; Olympus, Tokyo, Japan).

Measurement of the ATP content of oocytes

The ATP content of completely denuded oocyte was measured using a commercial assay based on the luciferin-luciferase reaction (Promega, Sunnyvale, Ca). Oocytes were rinsed three times in phosphate buffered saline (PBS), and then transferred individually in 50 uL of PBS into plastic tubes. Then, 50 uL of BacTiter-Glo reagent was added to all tubes were incubated for 5 min at room temperature. The ATP content of the samples was measured using a liminometer (Luminometer 20/20n, Promega) with high sensitivity (0.001 pmol). A five-point standard curve (0-10 pmole/tube) was routinely included in each assay. The ATP content was determined from the formula for the standard curve.

RESULTS AND DISCUSSION

Oxygen consumption of pig oocytes before and after *in vitro* maturation

Oxygen consumption rates of immature oocytes (immediately upon recovery from ovary) were 0.44×10^{14}/mol s⁻¹. In the maturation culture, a higher oxygen consumption rate was found in matured oocytes (with polar body extrusion), whereas the oxygen consumption rate of non-matured oocytes (without polar body extrusion) decreased during oocyte maturation (Table 1). These results showed that the oxygen consumption of pig oocytes changed in maturation status of oocytes.

Table 1. Oxygen consumption rates of pig oocytes in different maturaton status

Maturation status	O_2 consumption rate ($F \times 10^{14}$/mol · s⁻¹)
Immature	0.44 ± 0.03 [a]
Mature	0.44 ± 0.03 [a]
Non-mature	0.21 ± 0.03 [b]

Values with different superscripts in each column are significantly different ($P < 0.05$).

Distribution of mitochondria in pig oocytes

Mitochondrial localization in oocytes after IVM is showed in Figure 2. The oocytes were classified in three types (Type-I, Type-II or Type-III) according to the pattern of active mitochondria distribution. Staining with MitoTracker orange revealed small mitochondrial clumps that were as a rule found in the periphery of the cytoplasm (Type-I). The Type-II oocytes showed the strong and homogeneous staining. In the oocytes classified as Type-III, mitochondrial clumps showing the strongest staining were seen in the central parts of the cytoplasm. The number of Type-II and Type-III oocytes gradually increased during the maturation culture. These results suggest that active mitochondria moved from the periphery to the central parts of the cytoplasm in oocytes during oocyte maturation. Similar mitochondrial reorganization has been reported in bovine oocytes before and after IVM [21].
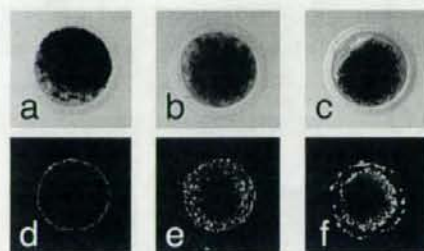

Fig. 2. Midline confocal sections of pig oocytes after maturation culture. a-c: Nomarski differential interference micrographs. d-f: Pig oocytes stained by MitoTracker orange. The oocytes are classified into three categories according to the mitochondria distribution, such as Type-I (a, d), Type-II (b, e), and Type-III (c, f).

Respiration rates and ATP content of different type of oocytes

The respiration rate and ATP content of Type-I oocyte were significantly lower than in Type-II and Type-III oocytes (Table 2). Although Type-II oocytes showed the high respiratory activity, they contained significantly less ATP than oocytes of Type-III oocytes. The average respiration rate and ATP content of Type-III

oocytes tended to be higher than that of other types of oocytes. These results demonstrated that the oxygen consumption rate and ATP content of pig oocytes was significantly affected by category of mitochondrial distribution. Type-II oocytes are thought to be an intermediate type between Type-I and Type-III oocyte in maturation status. This study suggests that there is a correlation between the respiratory activity and the maturation status of pig oocytes.

Table 2. Oxygen consumption rates of pig oocytes in different maturaton status

Category	O_2 consumption rate $(F \times 10^{14}/\text{mol} \cdot \text{s}^{-1})$	ATP content (pmol/oocyte)
Type-I	0.20 ± 0.10 [a]	0.08 ± 0.01 [a]
Type-II	0.54 ± 0.02 [b]	1.66 ± 0.11 [b]
Type-III	0.53 ± 0.01 [b]	2.08 ± 0.05 [c]

Values with different superscripts in each column are significantly different ($P < 0.05$).

CONCLUSIONS

In this study, oxygen consumption by single pig oocytes was non-invasively and quantitatively determine by SECM measuring system. The biochemical and cytological studies strongly suggest that oxygen consumption is an important parameter to evaluate the competence of oocyte maturation in the pig. SECM measuring procedures can be used to accurately evaluate the metabolic activity and quality of pig oocytes.

ACKNOWLEDGEMENTS

REFERENCES

[1] R.M. Mills and R.L. Brinster, *Exp. Cell Res.*, 47, 337-44 (1967).

[2] B. Nilsson, C. Magnusson, S. Widehn and T. Hillensjo, *J. Embryol. Exp. Morphol.*, 71, 75-82 (1982).

[3] C. Magnusson, T. Hillensjo, L. Hamberger and L. Nilsson, *Hum. Reprod.*, 1, 183-4 (1986).

[4] J.G. Thompson, R.J. Partridge, F.D. Houghton, C.I. Cox and H.J. Leese, *J. Reprod. Fertil.*, 106, 299-306 (1996).

[5] I. Donnay and H.J. Leese, *Mol. Reprod. Dev.*, 53, 171-8 (1999).

[6] J.R. Trimarchi, L. Liu, D.M. Porterfield, P.J.S. Smith and D.L. Keefe, *Biol. Reprod.*, 62, 1866-74 (2000).

[7] A.J. Bard and M.V. Mirkin,"Scanning Electrochemical Microscopy", Marcel Dekker Inc., New York (2000).

[8] K. Yamashita, M. Takagi, K. Uchida, H. Kondo and S. Takenaka, *Analyst*, 26, 1210-11 (2001).

[9] D. Oyamatsu, N. Kanaya,, H. Shiku, M. Nishizawa and T. Matsue, *Sens. Actuat. B: Chem.*, 91, 199-204 (2003).

[10] H. Shiku, T. Matsue and I. Uchida, *Anal. Chem.*, 68, 1276-8 (1996).

[11] S. Kasai, A.Z.H. Yokota, M. Nishizawa, K. Niwa, T. Onouchi and T. Matuse, *Anal. Chem.*, 72, 5761-5 (2001).

[12] H. Zhou, H. Shiku, S. Kasai, H. Noda, T. Matsue, H. Ohya-Nishiguchi and H. Kamada, *Bioelectrochemistry*, 54, 151-6 (2001).

[13] M. Nishizawa, K. Takoh and T. Matsue, *Langmuir*, 18, 3645-9 (2002).

[14] H. Shiku, T. Shiraishi, H. Ohya, T. Matsue, H. Abe, H. Hoshi and M. Kobayashi, *Anal. Chem.*, 73, 3751-8 (2001).

[15] H. Abe and H. Hoshi, *J. Reprod. Dev.*, 49, 193-202 (2003).

[16] H. Abe, H. Shiku, S. Aoyagi and H. Hoshi, *J. Mamm. Ova Res.*, 21, 22-30 (2004).

[17] L. Veek, *Ann. N.Y. Acad. Sci.*, 541, 259-74 (1988).

[18] H. Shiku, T. Shiraishi, S. Aoyagi, Y. Utsumi, M. Matsudaira, H. Abe, H. Hoshi, S. Kasai, H. Ohya and T. Matsue, *Anal. Biochim. Acta*, 522, 51-8 (2004).

[19] T. Matsue, S. Koike and I. Uchida, *Biochem. Biophys. Res. Commun.*, 197, 1283-7 (1993).

[20] P. Quinn, J.K. Kerin and G.M. Warnes, *Fertil. Steril.*, 44, 493-8 (1985).

[21] M. Stojkovic, S.A. Machado, P. Stojkovic, V. Zakhartchenko, P. Hutzler, P.B. Goncalves and E. Wolf, *Biol. Reprod.*, 64, 904-9 (2001).

Measurement of the Respiratory Activity of Single Human Embryos by Scanning Electrochemical Microscopy

Hiroyuki Abe[1*], Masaki Yokoo[2], Takahiro Itoh-Sasaki[1], Megumi Nasu[3], Kaori Goto[3], Yoko Kumasako[3], Yasuhisa Araki[4], Hitoshi Shiku[5], Tomokazu Matsue[5], Takafumi Utsunomiya[3]

[1*]Graduate Program of Human Sensing and Functional Sensor Engineering, Graduate School of Science and Engineering, Yamagata University, Yonezawa, Japan; [2]Innovation of New Biomedical Engineering Center, Tohoku University, Sendai, Japan; [3]St-Luke Clinic, Oita, Japan; [4]The Institute for ARMT, Gunma, Japan; [5]Graduate School of Environmental Studies, Tohoku University, Sendai, Japan

*To whom correspondence should be addressed Fax: 81-238-26-3361; e-mail: abeh@yz.yamagata-u.ac.jp

Respiration is useful parameter for evaluating embryo quality as it provides important information about metabolic activity. In the present study, we employed scanning electrochemical microscopy (SECM) to accurately determine the oxygen consumption of single, identical human embryos at different developmental stages. The oxygen consumption rates of single embryos were low at 2-8-cell stages ($0.51 \pm 0.05 \times 10^{14}$/mol $\cdot$ s^{-1}, n=18) but increased by the morula ($0.61 \pm 0.11 \times 10^{14}$ /mol $\cdot$ s^{-1}, n=5) and early blastocyst ($0.72 \pm 0.06 \times 10^{14}$/mol $\cdot$ s^{-1}, n=14) stages. Later blastocysts exhibited even higher oxygen consumption rates ($1.00 \pm 0.19 \times 10^{14}$/mol $\cdot$ s^{-1}, n=4). Ultrastructural studies revealed that most mitochondria in embryos up to the 8-cell stage were immature and had a spherical or ovoid shape. However, by the morula stage, the mitochondria had elongated cristae, with the elongated morphology even more pronounced in mitochondria present in blastocysts. The maturation of mitochondria correlated with the increase of oxygen consumption rate during the development of embryos. The SECM technique may be a valuable tool for accurately assessing the mitochondrial function and quality of human embryos.

Key words: cell respiration; electrochemical miscroscopy; human embryo; culture

INTRODUCTION

Embryo quality is an important determinant of the success of embryo transfer and accurate evaluation of embryo quality improves the pregnancy rate for assisted reproduction of mammals, including humans. Several approaches have been used to evaluate embryo quality and viability. Morphological evaluation is the primary method. However, morphological evaluation is subjective and difficult, especially for embryos with intermediate morphological qualities [1]. Therefore, more objective selection criteria are needed.

The metabolic activity of embryos has been determined from the consumption of nutrients, such as glucose, pyruvate and amino acids [2]. Oxygen consumption is an ideal indicator of overall metabolic activity because adenosine triphosphate (ATP) is generated predominantly by oxidative phosphorylation, a process in which oxygen plays an essential role [3]. In previous paper we describe a novel cell respiration measuring system, scanning electrochemical microscopy (SECM). This technique is a useful method for evaluating embryo quality that correlates metabolic respiration with morphological quality, developmental potential, and pregnancy rate following embryo transfer [4]. In this study, we employed SECM to accurately determine the oxygen consumption of single, identical human embryos at different developmental stages.

MATERIAL AND METHODS

Oocyte retrieval and embryo culture

Ovarian stimulation was performed using with human menopausal gonadotropin (HMG; Nikken Kagaku, Tokyou, Japan), gonadotropin-releaseing hormone (GnRH) agonist (Buserecur, Fujiseiyaku, Tokyo, Japan), using the extended protocol. Human chorionic gonadotropin (HCG; Profasi, Serono, Switzerland, 10,000IU) was administrated when the diameter of the dominant follicle was 20 mm. Transvaginal oocyte aspiration was performed 34 h after HCG was administrated.

Oocytes were inseminated by conventional *in vitro* fertilization

(IVF) by 3-4 h after oocyte retrieval. Following an IVF-embryo transfer (ET) procedure, surplus embryos that patients preferred not to keep preserved were designated for our study. Informed consent for use of embryos in research was obtained from all patients. The embryos were cultured in Sydney IVF Cleavage Medium (Cook IVF, Brisbane, Australia) until Day 3, after which they were cultured in Sydney IVF Blastocyst Medium (Cook IVF). Embryos were evaluated by the Veeck method [5] at early developmental stage (day 3 after IVF) and by the Gardner method [6] at blastocyst stage based on their morphological features.

Scanning electrochemical microscopy measuring system

In this study, oxygen consumption was measured by SECM procedure [7,8]. This modified SECM system includes a measuring instrument on an inverted optical microscope stage, a potentiostat (Hokuto Denko Co., Tokyo, Japan), and a notebook computer as controller and analyzer (Fig. 1a-d). Pt-microdisk electrodes sealed in a tapered soft-glass capillary (Fig. 1e) were fabricated according to the method [9]. The tip potential was held at -0.6V versus Ag/AgCl with a potentiostat to monitor the local oxygen concentration in the solution. For the measurement of oxygen consumption, HFF99 medium (Fuso Pharmaceutical Industries, Osaka, Japan) was employed. Voltammetry of the Pt-microdisk electrode in HFF99 medium showed a steady-state oxygen reduction wave. No response from other electrochemically active species was observed near the oocyte surface. The tip scanning rate was 31.1 µm/s. The microelectrode with a Pt-disk radius less than 3 µm was selected so that the oxygen reduction current of the electrode was less than 1.0 nA. To easily handle many oocytes in a short time, a plate with cone-shaped microwells was used (Fig. 1f). The single human embryo was transferred into a cone-shaped microwell filled with HFF99 medium and embryo fell to the bottom of the well and remained at the lowest point (Fig. 1g). The microelectrode was scanned according to the z-direction from side point of sample (Fig. 1g, h). The motor driven XYZ-stage was located on the microscope stage for electrode tip scanning. The XYZ stage and potentiostat were controled by computer. The oxygen consumption rate of embryos is calculated by newly designed software based on spherical diffusion theory [7]. Measurements of each embryo were performed very rapidly
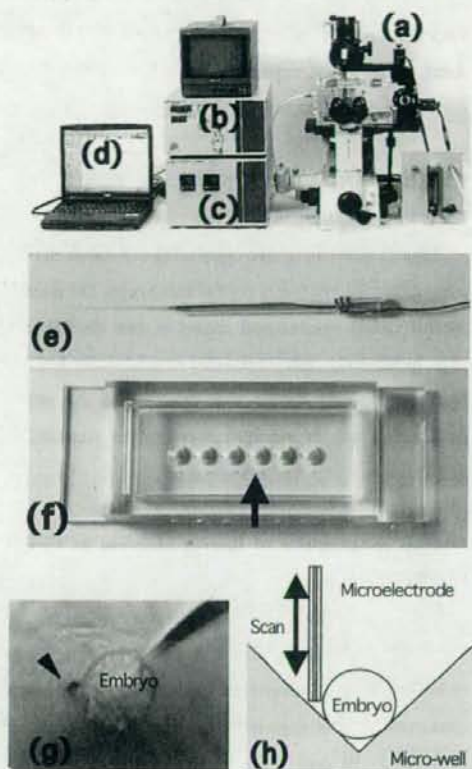
(within 1 min).

Fig. 1. A modified scanning electrochemical microscopy (SECM) system. SECM system includes a measuring instrument on the inverted optical microscope stage (a), potentiostat (b), controller (c), notebook computer (d), a microelectrode (e), and a plate (f) for measuring respiration activity of embryos. The plate has six cone-shaped microwells (arrow in f). Individual embryos are transferred into a microwell filled with medium. The embryo sinks down to the bottom of the well, remaining at the lowest point (g). Microelectrode (arrowhead in g) is scanned along the z-axis from the side point of embryo (h).

Electron microscopy

The electron microscopic study was carried out by the methods described previously [10]. Human embryos in various stages were fixed in 2.5% glutaraldehyde and postfixed in 1% osmium tetroxide in 0.1 M phosphate buffer (pH 7.4) for 1 h at 0-4 °C. Subsequently, the embryos were individually embedded in 1% agar. All samples were dehydrated by ethanol, substituted in

propylene oxide, and embedded in epoxy resin. Ultrathin sections were cut with a diamond knife on an ultramicrotome (Reichert Ultracuts, Leica, Heerbrugg, Switzerland), stained with uranyl acetate and lead citrate, and examined using a transmission electron microscope (JEM-1210, Jeol, Tokyo, Japan).

RESULTS AND DISCUSSION
Morphology of human embryos

Figure 2 shows the morphological features of human embryos using differential interference contrast microscopy. The embryos showed various morphological features in each developmental stage. In this study, embryos classified as good quality based on their morphological features were selected and the oxygen consumption rates of individual embryos were measured by SECM system.

Oxygen consumption of human embryos in various developmental stages

Using a modified SECM measuring procedure, we successfully measured the respiration activity of single human embryos at several developmental stages (Table 1). The oxygen consumption rates of single embryos were low at 2-8-cell stages $(0.51 \pm 0.05 \times 10^{14}/\text{mol} \cdot \text{s}^{-1}, n=18)$ but increased by the morula $(0.61 \pm 0.11 \times 10^{14}/\text{mol} \cdot \text{s}^{-1}, n=5)$ and early blastocyst $(0.72 \pm 0.06 \times 10^{14}/\text{mol} \cdot \text{s}^{-1}, n=14)$ stages. Later blastocysts exhibited even higher oxygen consumption rates $(1.00 \pm 0.19 \times 10^{14}/\text{mol} \cdot \text{s}^{-1}, n=4)$. These results demonstrate that SECM can detect differences in respiration activity of human embryos at several developmental stages.

The SECM system used in the present study can detect the oxygen concentration (ΔC) as small as a 1 μM difference between the bulk solution and the embryo surface; therefore, the system gives a precise and quantitative feature of oxygen consumption of single embryo [7]. Recently, SECM has been employed to quantify the respiration activity of embryos in several animal species [11]. SECM has been utilized to measure the respiration activity of single embryos from livestock, such as cattle and pigs, as well as those from small rodents, all with high reproducibility.

Ultrasructural features of mitochondria

Ultrastructural studies revealed that most mitochondria in

embryos up to the 8-cell stage are immature and have a spherical or ovoid shape (Fig. 3a). However, by the morula stage, mitochondria have elongated cristae (Fig. 3b). This morphology is even more pronounced in mitochondria present in blastocysts (Fig. 3c). These results demonstrated that the maturation of mitochondria correlates with an increase of oxygen consumption rates during the development of human embryos. Similar findings have been reported in bovine embryos [4]. Mitochondria exhibited specific morphological changes as the respiration activity increased, because the number of mitochodria per cell and the number of cristae per mitochondrion are related to the energy requirement by respiration [12].
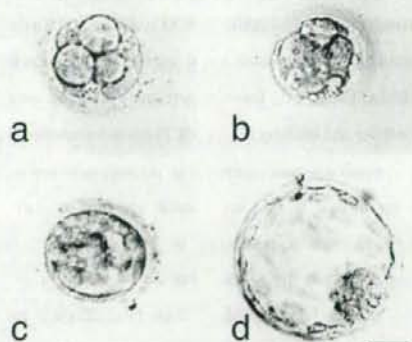

Fig. 2. Nomarski differential interference micrographs of 8-cell (a), morula (b), early blastocyst (c), and blastocyst (d) stages of human embryos developed from in vitro fertilized oocytes. Bar = 50 μm.

Table 1. Oxygen consumption rates of human embryos at various developmental stages

Embryonic stage	No. of embryos examined	O_2 consumption rate $(F \times 10^{14}/\text{mol} \cdot \text{s}^{-1})$
2-8 cell	18	0.51 ± 0.05 [a]
Morula	5	0.61 ± 0.11 [ab]
Early blastocyst	13	0.72 ± 0.06 [b]
Blastocyst	4	1.00 ± 0.19 [c]

Values with different superscripts in each column are significantly different $(P < 0.05)$.

Mitochondria contribute a vital role to the metabolism of

energy-compounds in the cytoplasm to provide ATP for embryonic development. The development of mitochondria may be an important factor in embryo quality. There are conspicuous differences in the ultrastructural features of bovine embryos of high and low quality [13]. Morulae classified as low quality by morphological classification contained nucleoli with low transcriptional activity, a large number of lipid droplets, and immature mitochondria, consistent with these low quality embryos displaying low metabolic activities, including oxygen consumption. Thus, oxygen consumption associated with mitochondrial development is a reliable indicator of embryo quality.
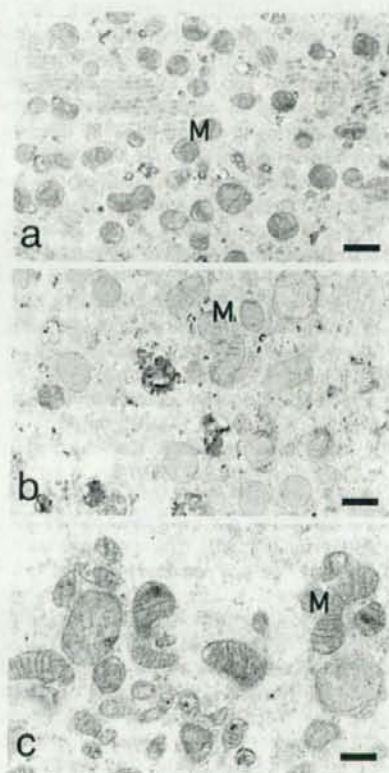

Fig. 3. Electron micrographs of human embryos at 2-cell (a), morula (b), and blastocyst (c). M, mitochondria. Bars = 0.5 μm.

CONCLUSIONS

SECM can non-invasively measure oxygen consumption by single, identical human embryos. This technique is a valuable tool for accurately assessing the mitochondrial function of human embryos. As respiration activity correlates with the quality of embryos, this technique may contribute to assessing the quality of human embryos in *in vitro* fertilization clinics.

REFERENCES

[1] I. Boiso, A. Veiga, R.G. Edwards, *Reprod. Biomed. Online,* 5, 328-50 (2002).

[2] D. Rieger ,*Theriogenology,* 37, 75-93 (1992).

[3] J.R. Trimarchi, I. Liu, D.M. Porterfield, P.J.S. Smith, D.L. Keefe, *Biol. Reprod.,* 62, 1866-74 (2000).

[4] H. Abe, H. Shiku, M. Yokoo, S. Aoyagi, S. Moriyasu, A. Minamihashi, T. Matsue, H. Hoshi, *J. Reprod. Dev.,* 52 (Suppl.), S55-64 (2006).

[5] L.L. Veek, *"Atlas of the human oocyte and early conceptus,* Vol. 2. Williams & Wilkins Co, Baltimore (1991)

[6] D.K. Gardner, W.B. Scoolcraft, Jansen R., *"In vitro culture of human blastocysts"*, Eds. by R. Jansen, D. Mortimer, Carnforth, Parthenon Press (1999) pp. 378-89.

[7] H. Shiku , T. Shiraishi, H. Ohya, T. Matsue, H. Abe, H. Hoshi, M. Kobayashi, *Anal. Chem.,* 73, 3751-58 (2001).

[8] H. Abe, H. Shiku, S. Aoyagi, H. Hoshi, *J. Mamm. Ova Res.,* 21, 22-30 (2004).

[9] T. Matsue, S. Koike and I. Uchida, *Biochem. Biophys. Res. Commun.,* 197, 1283-7 (1993).

[10] H. Abe, S. Yamashita, T. Satoh, H. Hoshi, *Mol. Reprod. Dev.,* 61, 57-66 (2002).

[11] H. Abe, *J. Mamm. Ova Res.,* 24, 70-78 (2007).

[12] D.W. Fawcett, Mitochondria, *"The Cell"*, Philadelphia, Saunders Company (1981) pp. 410-88.

[13] H. Abe, S. Matsuzak, H. Hoshi, *Theriogenology,* 57, 1273-83 (2002).

Morphometric and Ultrastructural Changes in Ciliated Cells of the Oviductal Epithelium in Prolific Chinese Meishan and Large White Pigs during the Oestrous Cycle

H Abe[1] and H Hoshi[2]

[1]*Tohoku University Biomedical Engineering Research Organization (TUBERO), Sendai, Japan;* [2]*Research Institute for the Functional Peptides, Yamagata, Japan*

Contents

There are some differences in reproductive features between the Chinese Meishan (CM) pig and Large White (LW) pig. The aim of the present study was to investigate the quantitative changes and ultrastructural features of ciliated cells in the various regions of the CM and LW pig oviduct during the follicular and luteal phases of the oestrous cycle. In the fimbrial and ampullar epithelia at the follicular phase, the ciliated cells were more plentiful than in the isthmic region in both pigs. In the CM pigs, there was a striking decrease in the percentage and cell height of ciliated cells in the luteal phase compared with the follicular phase. Although similar quantitative changes were observed in the LW pig oviduct, these changes were less dramatic than that in the CM pig oviduct. In both pigs, the percentage and cell height of ciliated cells in the isthmus were unchanged between the follicular and luteal phases. The ultrastructure of ciliogenic and ciliated cells was observed. In the fimbrial and ampullar epithelia during the follicular phase, most of the ciliated cells showed normal morphology, having many elongated cilia and mitochondria, but in the CM pig oviduct during the luteal phase many of the ciliated cells possessed immature cilia and swollen mitochondria. Cells undergoing ciliogenesis were frequently observed in the fimbriae and ampulla, and occasionally in the isthmus. Cytoplasmic protrusions containing variable numbers of ciliary axonemal complexes occurred in the fimbrial and ampullar epithelium in the CM pigs at the luteal phase, suggesting that deciliation of cells occurs by membrane-bound cilia packets forming at the apices of cells and pinching off. These results demonstrate that there are regional variations in the cyclic changes associated with the oviductal ciliated cells of the pigs, while there are marked morphometrical and ultrastructural changes in oviductal ciliated cells of the CM pigs compared with that of the LW pigs.

Introduction

The epithelium of the oviduct consists of two types of cell: ciliated and nonciliated secretory cells. The ciliated cells may play an important role in the transport of oocytes and embryos (Odor and Blandau 1973) and possibly in the regulation of sperm progression (Hunter et al. 1991). On the other hand, the secretory cells produce and release specific secretory materials which may play important roles in embryonic development and sperm function (Hunter 1994; Abe et al. 1995; Gandolfi 1995). These cells undergo marked morphological and functional changes in association with fluctuations of the ovarian hormones during the oestrous cycle (Rumery et al. 1978; Odor et al. 1980). Moreover, it is known that the oviductal epithelial cells show marked regional variations in ultrastructural, histo-

chemical, biochemical, and physiological features in many mammals (Abe 1996).

The Chinese Meishan (CM) pig is known as a precocious and prolific breed (Cheng 1984). It has been reported that there are differences in rates of ovulation, embryo-placental development, and the size of the uterus between the Large White (LW) pig and the CM pig (Bazer et al. 1988a,b). In particular, it seems that the reproduction success of the CM pig is associated with higher rates of embryo development. Therefore, it is of great interest to compare the ultrastructural features of oviductal epithelial cells between the CM pig and the LM pig. In previous studies, it has been described the ultrastructural features of epithelial cells in the LW pig oviduct (Nayak et al. 1976a,b, 1976c, 1977). The surface morphology of oviductal epithelium has been investigated in LW pigs (Stalheim et al. 1975; Wu et al. 1976; Yaniz et al. 2006). Similarly, the luminal surfaces of epithelial cells in various regions of the oviducts of CM pigs were examined by scanning electron microscopy (Abe and Oikawa 1992). However, available information on the reproductive tracts, including the oviduct of CM pig, is still limited.

Recently, we have reported the marked regional changes in the ultrastructural features of secretory cells in the CM pig oviduct, which are associated with the stages of the oestrous cycle (Abe and Hoshi 2007). This study provides insight into the regional and cellular differences in functions of secretory cells of the CM pig oviduct. Therefore, it is important to investigate how cytomorphometric and ultrastructural changes of ciliated cells occur in the CM pig oviduct during the oestrous cycle. The objective of the current study was to: (i) quantitate the numbers and heights of ciliated cells, (ii) examine the ultrastructure of the ciliogenic and ciliated cells present in the fimbrial, ampullar, and isthmic epithelium of the oviduct at the follicular and luteal phase of the oestrous cycle and (iii) compare these morphological features between the CM pig and the LW pig.

Materials and Methods

Sexually mature CM pigs and LW pigs were observed at least twice per day for evidence of oestrus before they were placed into an experiment. Two groups of three CM pigs and five LM pigs at different stages of the oestrous cycle (day 1 and days 10–14) were killed at a local meat processing plant. Day 1 refers to the day of

onset of oestrus (follicular phase), and days 10–14 refer to the late dioestrus (luteal phase). The stages of the cycle were confirmed by careful examination of the ovaries according to the previous method (Akins and Morrissette 1968). They were destinated to the food chain after slaughter.

Oviductal segments were processed for transmission electron microscopy according to our previous study (Abe and Oikawa 1992). Oviducts were recovered within 20 min of slaughter. After the oviduct had been trimmed of fat and extraneous tissue, the fimbriae, ampulla, and isthmus were cut apart. Strips of tissue were cut along the borders of the fimbrial folds and the luminal ridges of the ampulla and isthmus. These tissues were fixed by immersion in 2% paraformaldehyde (PA)-2.5% glutaraldehyde (GA) for 3 h. After fixation, the segments were trimmed into small pieces and fixed again for 3 h in 2% PA-2.5% GA. The pieces of tissue were postfixed for 2 h with 1% osmium tetroxide. All fixatives were prepared in 0.1 M phosphate buffer (pH 7.4) and tissues were rinsed after fixation in phosphate buffer. All fixation and rinsing steps were carried out at 0–4°C. Osmolality of PA-GA fixative was approximately 400 mOsm. After fixation, the oviducts were dehydrated in ascending concentrations of ethanol, and embedded in Epon 812 resin (Taab Laboratories Equipment Ltd, Berkshire, UK). All sections were prepared using an ultramicrotome (NOVA, Pharmacia LKB, Uppsala, Sweden). Semithin sections were cut with a glass knife and ultrathin sections were cut with a diamond knife. Semithin sections were placed on glass slides, stained with 1% toluidine blue and examined under a light microscope (BH2: Olympus Optical Co., Ltd, Tokyo, Japan). Ultrathin sections were stained with uranyl acetate and lead citrate and examined using a transmission electron microscope (JEM-100SX, Jeol, Tokyo, Japan) operated at 60 kV.

To obtain quantitative data on the percentage of ciliated cells, 1.5 μm semithin sections of cells were examined under the light microscope as in the method described previously (Abe and Oikawa 1992). The percentages of ciliated cells were determined by scanning 250–500 cells per block from at least three different blocks of fimbriae, ampulla, and isthmus per animal. All the epithelial cells that extended as far as the luminal surface were counted, while those in obliquely cut areas were excluded. The height of epithelial cells and the length of cilia were measured with an ocular micrometer. For these measurements we selected, in each region, 75–125 ciliated cells in which the plane of the section clearly passed through the cell nucleus, parallel to the longitudinal axis of the cell. Each result is expressed as the mean ± standard error of the mean.

Statistical analyses were performed using one-way analysis of variance (ANOVA, Abacus Concepts, Stat-View, Berkeley, CA, USA) and Fisher's protected least significant differences test.

Results

Figure 1 shows the morphology of the mucosa in the three regions of CM pig oviduct during both the follicular and luteal phases of the oestrous cycle. In the epithelium of all regions, two distinct cell types, ciliated and nonciliated (secretory) cells were distinguished. During the follicular phase, ciliated cells were predominate in the fimbrial epithelium (Fig. 1a). Basophilic granules were present in the apical cytoplasm of
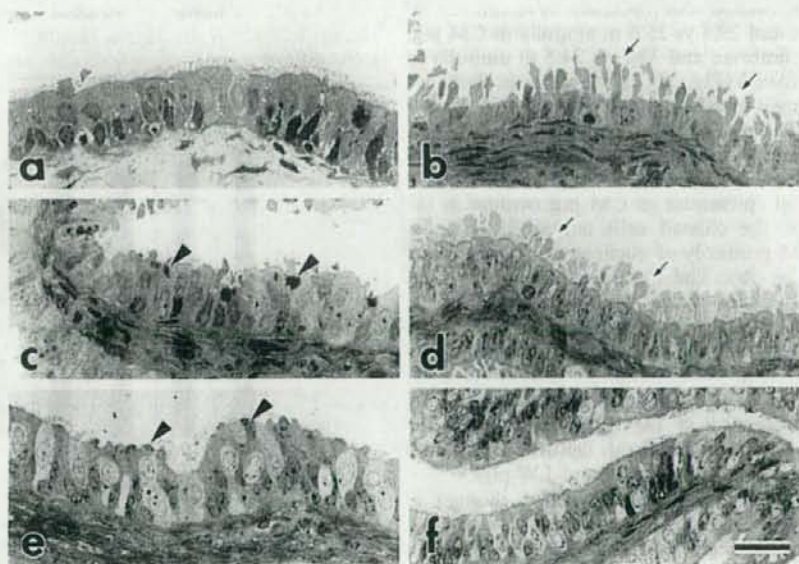

Fig. 1. Light micrographs of Chinese Meishan pig oviduct in cross-section showing the fimbriae (a, b), ampulla (c, d), and isthmus (e, f). (a, c, e) Follicular phase. (b, d, f) Luteal phase. Basophilic granules (arrowheads) are found in nonciliated cells in the ampulla (c) and isthmus (e) in the follicular phase. The cells are extended from the epithelium (arrows in b,d) in the luteal phase. Bar 20 μm

nonciliated cells in the ampulla and isthmus in the follicular phase (Fig. 1c, e). The apices of nonciliated cells showed various degree of protrusion. The protrusions extended beyond the tips of the cilia in the epithelium of the fimbriae (Fig. 1b) and ampulla (Fig. 1d) in the luteal phase. The epithelium of all oviductal regions in LW pig appeared similar to that in CM pig (not shown).

Figure 2 shows the mean percentage of ciliated cells and the cell height of ciliated and nonciliated cells in the oviductal epithelium of the fimbriae, ampulla, and isthmus during the follicular and luteal phases of the oestrous cycle. In CM pig, the mean percentage of ciliated cells significantly decreased from 81.1% in the fimbriae and 61.2% in the ampulla in the follicular phase to 31.0% and 39.7%, respectively in the luteal phase (Fig. 2a). Although the mean percentage of ciliated cells in LW pig oviduct significantly decreased from 80.5% in the fimbriae in the follicular phase to 74.7% in the luteal phase, this reduction was less dramatic than that in CM pig oviduct. The percentage of ciliated cells in the ampulla of LW pig oviduct was not significantly different between the follicular and luteal phases, 61.2% and 61.9%, respectively. In the isthmus, the drastic changes in percentage of ciliated cells were not observed between the follicular and luteal phases (34.0% and 34.4% in CM pig; 35.0% and 38.7% in LW pig, respectively). In both pigs, the height (μm) of ciliated cells in the epithelium of fimbrial and ampullar regions was dramatically reduced in the luteal phase compared with the follicular phase (follicular vs luteal: 29.7 vs 15.7 in fimbriae and 27.9 vs 16.4 in ampulla in CM pig; 30.3 vs 18.4 in fimbriae and 31.7 vs 17.4 in ampulla in LW pig, respectively) (Fig. 2b). The height of nonciliated cells was reduced in the epithelium in these two regions, although the reductions were less dramatic than those in the ciliated cells (follicular vs luteal: 32.7 vs 26.8 in fimbriae and 29.5 vs 25.6 in ampulla in CM pig; 30.5 vs 25.6 in fimbriae and 32.5 vs 24.8 in ampulla in LW pig, respectively) (Fig. 2c). In the isthmus, there are no marked changes in the height of ciliated (follicular vs luteal: 28.0 vs 26.8 in CM pig; 29.3 vs 27.7 in LW pig, respectively) and nonciliated (follicular vs luteal: 30.4 vs 28.3 in CM pig; 30.2 vs 28.8 in LW pig, respectively).

In the fimbrial epithelium of CM pig oviduct in the follicular phase, the ciliated cells contained indented nuclei composed primarily of euchromatin and distinct nucleoli (Fig. 1a, 3a). The mature ciliated cells were characterized by cilia, basal bodies, and an apical distribution of numerous mitochondria. Many of the mitochondria were long and oriented parallel to the long axis of the cell (Fig. 3b). Numerous polysomal complexes were scattered throughout the cytoplasm. Many mature cilia protruded at the apical surface of the ciliated cells. The ultrastructural features of mature ciliated did not differ between CM and LW pigs.

During the luteal phase, some marked changes in ultrastructural features were observed in the ciliated cells of the fimbrial region in the MS pig oviduct. In general, most ciliated cells had low electron density cytoplasm compared with that of the nonciliated cells (Fig. 3c). The nuclei of many cells showed ovoid structures and were composed of more prominent
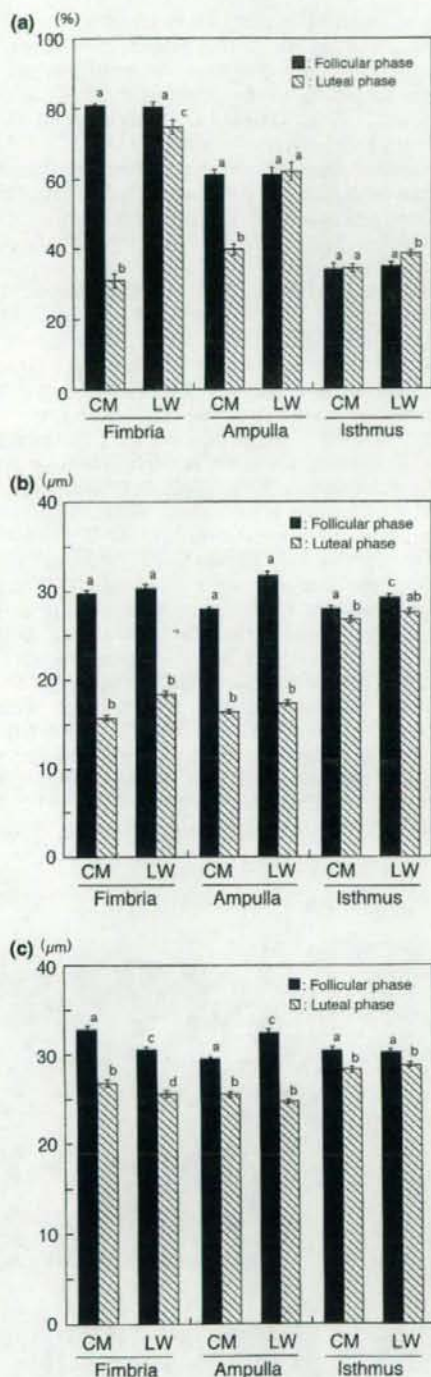

Fig. 2. Cyclic and segmental variations in proportion (a) and cell height of ciliated cells (b) and nonciliated cells (c) in the epithelium at the fimbrial, ampullar, and isthmic regions of the Chinese Meishan (CM) and Large White (LW) pig oviducts. Values are expressed as mean ± SEM (proportion: n = 9, cell height: n = 79–125). Values with different superscripts in each column (oviductal segment) differ significantly (p < 0.05)
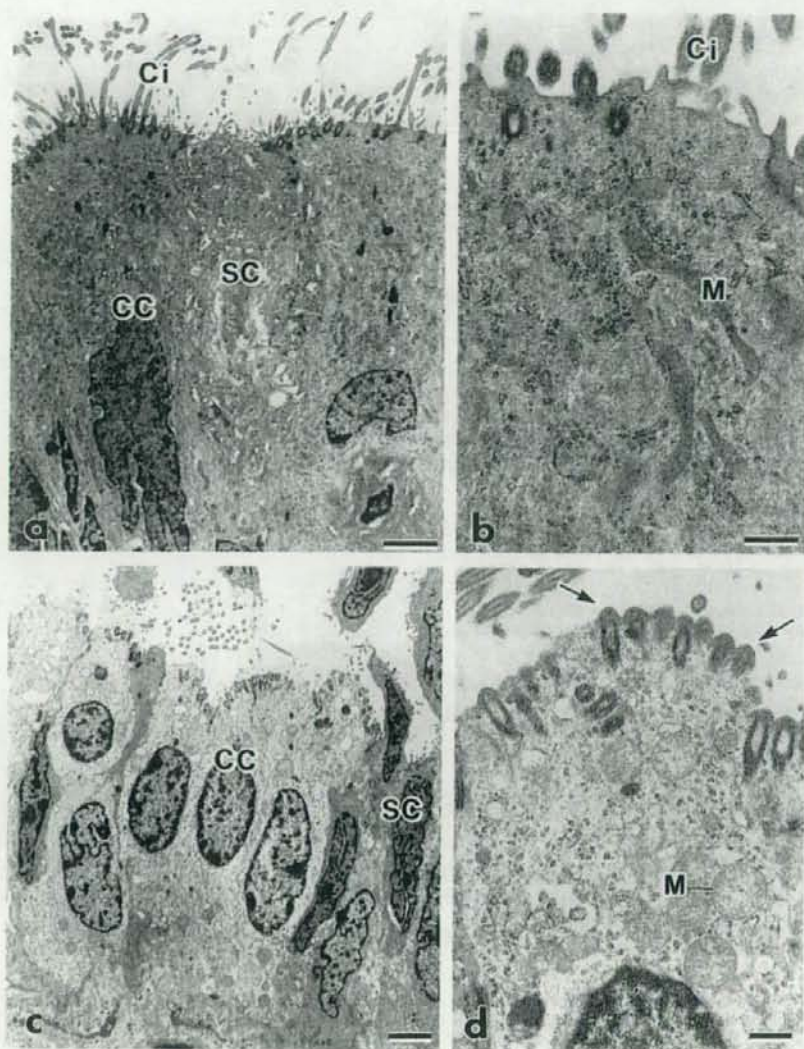
Fig. 3. Fimbrial epithelial cells of Chinese Meishan pig oviducts at follicular (a, b) and luteal (c, d) phases of the oestrous cycle. (a, b) The fimbrial ciliated cells have many mature cilia (Ci) and elongated mitochondria (M). (c, d) During the luteal phase, ciliated cells (CC) have low electron-dense cytoplasm and many short cilia (arrows). Many swollen mitochondria are seen in the supranuclear cytoplasm. BL, basal lamina; SC, secretory cells. Bars a, c = 2 μm; b, d = 0.5 μm

heterochromatin at the peripheral margins of the nuclear membrane compared with the follicular phase. The cilia were shorter than those in the follicular phase and these immature cilia had a characteristic blunt tip (Fig. 3d). Most mitochondria had a round shape. In the ampulla and isthmus, the mature ciliated cells showed similar ultrastructural features to the fimbrial ciliated cells. These ciliated cells possessed a nucleus with nucleoli and condensed chromatin, cilia, basal bodies, and elongated mitochondria, and there were no dramatic ultrastructural changes as were observed in the fimbriae during the luteal phase (not shown).

Cells demonstrating ciliogenesis were observed with moderate frequency in the epithelium of the fimbriae and occasionally in the ampulla and isthmus. The frequency of appearance of ciliogenic cells was higher in the follicular phase than in the luteal phase. In these ciliogenic cells, many fibrous granules, which were small and round, and electron-dense granules without a limiting membrane, were observed in the area between the nucleus and the apex of cell (Fig. 4a). Also, several deuterosomes, which were of higher electron density than the fibrous granules, occurred near aggregates of the fibrous granules. The deuterosomes were classified into two types. One type appeared spherical and solid, 0.1–0.2 μm in diameter, while the other appeared hollow, and 0.2–0.5 μm in diameter (Fig. 4a, inset). Procentrioles arose around the deuterosomes in
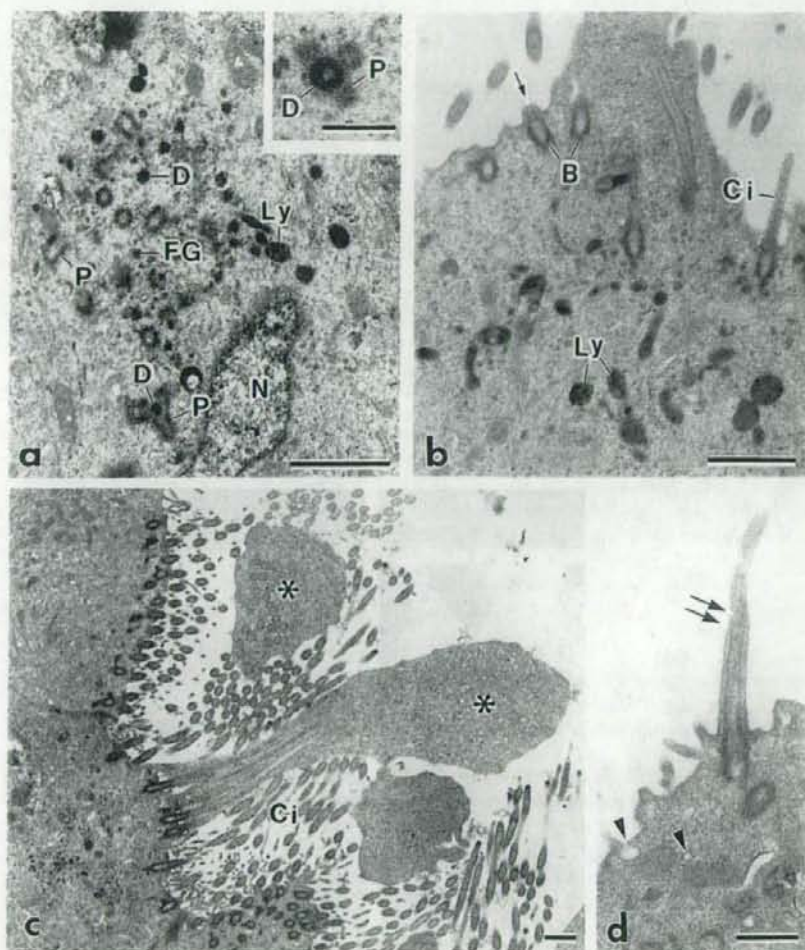
Fig. 4. Apical portions of epithelial cells of the Chinese Meishan pig oviduct. (a, b) Ciliogenic cells. Aggregates of fibrous granules (FG) around deuterosomes (D) are seen in the supranuclear cytoplasm. The insertion illustrates a hollow deuterosome. Procentrioles (P) are located around the deuterosome in a spoke-like arrangement. Some lysosome-like bodies (Ly) are seen around the deuterosome and procentrioles. Basal bodies (B) are forming cilia and small bulge (arrow) in the cell membrane is seen (arrow). (c) Ciliated cells of the fimbrial epithelium. Cytoplasmic protrusions (asterisks) contain internalized parts of ciliary axonemes. (d) An epithelial cell illustrating the presence of a solitary cilium (SC). Notice the small endocytotic vesicles (arrowheads). Bars a, b, c = 1 μm; d, Inset in a = 0.5 μm

a spoke-like formation and developed into basal bodies. Usually, one deuterosome was associated with one to six procentrioles. The basal bodies migrated from near the aggregates of fibrous granules to the apical surface of the cell and there initiated the formation of cilia (Fig. 4b). As a result, ciliary buds were formed and each of them induced formation of a small bulge in the cell membrane, which eventually induced elongation of the cell membrane around the developing cilium. Sometimes, an irregular cytoplasmic process surrounding the elongating cilium was observed. In the fimbrial epithelium, irregular cytoplasmic protrusions were frequently observed in the mature ciliated cells at the luteal phase. Most of the protrusions were free of cellular organelles but contained internalized parts of ciliary axonemes (Fig. 4c). In some cells, a solitary cilium projected into the lumen and small vesicles that

appeared to be endocytotic vesicle were observed in the apical cytoplasm (Fig. 4d).

Discussion

This study demonstrates that the oviductal epithelium of the CM pig and LM pig undergoes a drastic change in ciliation during the oestrous cycle. Large numbers of ciliated cells were present in the epithelium of fimbriae and ampulla during the follicular phase, while the numbers of ciliated cells was significantly reduced in the luteal phase. Moreover, the height of the ciliated cells decreased noticeably in the luteal phase. These changes were particularly dramatic in the fimbriae. Similar observations have been described in the oviduct of the domestic animals (Abe and Oikawa 1993b; Abe et al. 1993). Cilia are thought to be primarily responsible for

the pickup and transport of ovulated eggs in the fimbriae, and the cilia of the ampullar epithelium have a similar function (Odor and Blandau 1973). A richly ciliated epithelium at ovulation (follicular stage) is important. It seems that the cyclic changes observed in the present study reflect the function of the cilia in the fimbriae and ampulla of the pig oviduct.

In the present cytomorphometric study, the numbers of ciliated cells in the pig oviductal epithelium, especially in the CM pig oviduct, significantly decreased in the fimbrial and ampullar regions at the luteal phase. Similar changes in ciliation have been observed in the primate oviducts (Rumery et al. 1978; Odor et al. 1980; Brenner et al. 1983). In the oviduct of the rhesus monkey, Brenner (1969a,b) demonstrated that large numbers of cilia are formed during the follicular phase, creating a richly ciliated epithelium, and extensive atrophy and deciliation take place during the luteal phase of the menstrual cycle. Deciliation is associated with a 'pinching off' of the apical portion of each ciliated cell (Brenner 1969a). Similar findings have been described in the oviduct of the pig-tailed monkey (Odor et al. 1980). In our previous study using scanning electron microscopy, 'pinching off' of the apical portions of epithelial cells was frequently observed in the CM pig oviduct (Abe and Oikawa 1992). The present study demonstrated that these apical protrusions contained internalized parts of ciliary axonemes. These findings suggest that the reduction in number of ciliated cells in the luteal phase may be accomplished by shedding of the cilia into the oviductal lumen.

The cells showing ciliogenesis were found in the fimbrial and ampulla epithelia during the oestrous cycle. The ultrastructural features of ciliogenesis observed in the CM pig oviductal epithelium were similar to those described in the oviducts of other species (Anderson and Brenner 1971; Dirksen 1971; McCarron and Anderson 1973; Komatsu and Fujita 1978b; Abe and Oikawa 1989). The initial event in ciliogenesis is the appearance of fibrous granules in the apical cytoplasm of the future ciliated cells. These fibrous granules are also called proliferative elements (Dirksen and Crocker 1965) and procentriole precursors or axonemal precursors (Steinman 1968). The second event in ciliogenesis is the appearance of electron-dense spherical bodies, designated deuterosomes (Sorokin 1968), within the aggregation of fibrous granules. The procentrioles begin to form shortly after or simultaneously with the appearance of fibrous granules and deuterosomes, and each procentriole usually develops in contact with the deuterosomes. Eventually, procentrioles lengthen, break away from the deuterosome, migrate toward the cell surface, and then each centriole becomes associated with the cell membrane to form a ciliary bud, which grows into a cilium. In the ciliogenic cells present in the oviductal epithelium of the CM pig, the deuterosomes were distinguished into two types, solid and hollow. The hollow type has never been observed in the monkey oviduct (Anderson and Brenner 1971), but both solid and hollow deuterosomes have been seen in the oviduct of the mouse (Komatsu and Fujita 1978a) and golden hamster (Abe and Oikawa 1989). It is not clear whether deuterosomes are actually utilized in the formation of the procentriole or whether they act merely as organizers for the generation of the procentriole.

The ciliated cells of the isthmus showed few changes between the follicular and luteal phases, in contrast to those of the fimbriae and ampulla. It has been suggested that the isthmic epithelial cells act as a sperm reservoir (Hunter et al. 1991). That study demonstrated specific and active interactions between the tips of the cilia and the flagella of bull spermatozoa in the caudal isthmus of the oviduct of cows, suggesting that the cilia in the oviductal isthmus may regulate contacts with spermatozoa flagella. In addition, some studies suggest that isthmic epithelial cells may have the ability to maintain the viability and fertilizing capacity of spermatozoa (Smith et al. 1987; Pollard et al. 1991; Suarez et al. 1991). However, the main function of isthmic ciliated cells of the mammalian oviduct remains unresolved.

The cytomorphometric analysis and transmission electron microscopy data of the present study revealed that there were marked regional differences in epithelial cells of the pig oviduct during cyclic changes. Although the reason for the regional differences is unclear, these regional differences may reflect regional variations in sensitivity to ovarian steroid hormones. Many studies have demonstrated that cytodifferentiation of epithelial cells of the oviduct is closely related to the effects of ovarian steroid hormones (Brenner et al. 1974; Verhage and Brenner 1975; Odor et al. 1980; Abe and Oikawa 1993a). In addition, it has been suggested that the regular cycle of ciliogenesis and deciliation by the epithelial cells of the mammalian oviduct is dependent upon the levels of circulating estrogen and progesterone (Brenner et al. 1974; Verhage et al. 1979; Abughrien and Dore 2000). Ciliogenesis in the follicular phase occurs under the influence of estrogen, while the appearance of progesterone at midcycle suppresses ciliogenesis and leads to deciliation. Moreover, it has been suggested by others that oviductal epithelial cells show regional differences in their responses to steroid hormones (Gupta et al. 1969; Fredricsson and Holm 1974; Bajpai et al. 1977). These findings strongly support our hypothesis that there are regional differences in the responses to hormones of epithelial cells in the various regions of the Chinese Meishan pig oviduct.

A solitary or single cilium, also designated a rudimentary or temporary cilium, was frequently observed in the CM pig oviductal epithelial cells in the luteal phase. Odor and Blandau (1985) observed such solitary cilia more frequently in the oviductal epithelium of ovariectomized and ovariectomized/progesterone-treated rabbits than in controls. Also, solitary cilia have been found on undifferentiated epithelial cells of neonatal oviducts (Komatsu and Fujita 1978a; Odor and Blandau 1985; Abe and Oikawa 1989). These findings suggest that the appearance of solitary cilia may be closely related to fluctuations in levels of ovarian hormones.

In summary, ciliated cells predominate in the fimbria and ampulla of the pig oviducts at the follicular phase of the oestrous cycle, and the numbers and height of ciliated cells is dramatically reduced in the luteal phase. The 'pinching off' of clusters of cilia from the ciliated cells of the fimbriae and ampulla of the CM pig oviduct

appears to be the mechanism for deciliation. Moreover, marked regional variations in ciliation were associated with the cyclic changes. These cytomorphometric and ultrastructural changes were more dramatic in the CM pig than those in the LW pig. Although the reason for these differences between the CM and LW pigs is unclear, it appears that there is a certain relation between the dramatic cyclic changes of oviductal epithelial cells and the prolific breed capacity of CM pig. The biological significance of regional and cyclic variations in ciliation of the CM pig oviduct needs further investigation to improve our understanding of the physiological function of oviductal epithelial cells in the reproductive process.

References

Abe H, 1996: The mammalian oviductal epithelium: Regional variations in cytological and functional aspects of the oviductal secretory cells: Histol Histopathol **11**, 743–768.

Abe H, Hoshi H, 2007: Regional and cyclic variations in the ultrastructural features of secretory cells in the oviductal epithelium of the Chinese Meishan pig: Reprod Domest Anim **42**, 292–298.

Abe H, Oikawa T, 1989: Differentiation of the golden hamster oviduct epithelial cells during postnatal development: an electron microscopic study: J Exp Zool **252**, 43–52.

Abe H, Oikawa T, 1992: Examination by scanning electron microscopy of oviductal epithelium of the prolific Chinese Meishan pig at follicular and luteal phases: Anat Rec **233**, 99–408.

Abe H, Oikawa T, 1993a: Effects of estradiol and progesterone on the cytodifferentiation of epithelial cells in the newborn golden hamster: Anat Rec **235**, 390–398.

Abe H, Oikawa T, 1993b: Observations by scanning electron microscopy of oviductal epithelial cells from cows at follicular and luteal phases: Anat Rec **235**, 399–410.

Abe H, Onodera M, Sugawara S, 1993: Scanning electron microscopy of goat oviductal epithelial cells at the follicular and luteal phases of the oestrous cycle: J Anat **183**, 415–421.

Abe H, Sendai Y, Satoh T, Hoshi H, 1995: Bovine oviduct-specific glycoprotein is a potent factor for the maintenance of the viability and motility of bovine spermatozoa *in vitro*: Mol Reprod Dev **42**, 226–232.

Abughrien BA, Dore MA, 2000: Ciliogenesis in the uterine tube of control and superovulated heifers: Cells Tissues Organs **166**, 338–348.

Akins EL, Morrissette MC, 1968: Gross ovarian changes during estrous cycle of swine: Am J Vet Res **29**, 1953–1957.

Anderson RGW, Brenner RM, 1971: The formation of basal bodies (centrioles) in the rhesus monkey oviduct: J Cell Biol **50**, 10–34.

Bajpai VK, Shipstone AC, Gupta DN, Karkun JN, 1977: Differential response of the ampullary and isthmic cells to ovariectomy and estrogen treatment: An ultrastructural study: Endokrinologie **69**, 11–20.

Bazer FW, Thatcher WW, Martinat-Botte F, Terqui M, 1988a: Conceptus development in Large White and prolific Chinese Meishan pigs: J Reprod Fertil **84**, 37–42.

Bazer FW, Thatcher WW, Martinat-Botte F, Terqui M, 1988b: Sexual maturation and morphological development of the reproductive tract in Large White and prolific Chinese Meishan pigs: J Reprod Fertil **83**, 723–728.

Brenner RM, 1969a: The biology of oviductal cilia. In: Hafez ESE, Blandau RJ, Hafez ESE, Blandau RJ (eds), The Mammalian Oviduct. The University of Chicago Press, Chicago and London, pp. 203–229.

Brenner RM, 1969b: Renewal of oviduct cilia during the menstrual cycle of the rhesus monkey: Fertil Steril **20**, 599–611.

Brenner RM, Resko JA, West NB, 1974: Cyclic changes in oviductal morphology and residual cytoplasmic estradiol binding capacity induced by sequential estradiol-progesterone treatment of spayed rhesus monkeys: Endocrinology **95**, 1094–1104.

Brenner RM, Carlisle KS, Hess DL, Sandow BA, West NB, 1983: Morphology of the oviducts and endometria of cynomolgus macaques during the menstrual cycle: Biol Reprod **29**, 1289–1302.

Cheng P-L, 1984: A highly prolific pig breed of China – The Taihu pig. Part III and IV: Pig News Inf **5**, 13–18.

Dirksen ER, 1971: Centriole morphogenesis in developing ciliated epithelium of the mouse oviduct: J Cell Biol **51**, 286–302.

Dirksen ER, Crocker TT, 1965: Centriole replication in differentiating ciliated cells of mammalian respiratory epithelium. An electron microscopic study: J Microsc **5**, 629–644.

Fredricsson B, Holm S, 1974: Dissociated response of the epithelium of the rabbit oviduct to estrogen: Biol Reprod **11**, 40–49.

Gandolfi F, 1995: Functions of proteins secreted by oviduct epithelial cells: Microsc Res Tech **32**, 1–12.

Gupta DN, Karkun JN, Kar AB, 1969: Studies on physiology and biochemistry of the Fallopian tube: response of the different parts of the rabbit Fallopian tube to estrogen and progesterone: Acta Biol Med Ger **22**, 551–559.

Hunter RHF, 1994: Modulation of gamete and embryonic microenvironments by oviduct glycoproteins: Mol Reprod Dev **39**, 176–181.

Hunter RHF, Flechon B, Flechon JE, 1991: Distribution, morphology and epithelial interactions of bovine spermatozoa in the oviduct before and after ovulation: A scanning electron miscroscope study: Tissue Cell **23**, 641–656.

Komatsu M, Fujita H, 1978a: Electron-microscopic studies on the development and aging of the oviduct epithelium of mice: Anat Embryol **152**, 243–259.

Komatsu M, Fujita H, 1978b: Some observations on ciliogenesis in the oviduct epithelium of the mouse: Arch Histol Jpn **41**, 229–237.

McCarron LK, Anderson E, 1973: A cytological study of the postnatal development of the rabbit oviduct epithelium: Biol Reprod **8**, 11–28.

Nayak RK, Alberts EN, Kassira WN, 1976a: Fine structural changes of the porcine uterine tube epithelium during early and late pregnancy: Am J Vet Res **37**, 1421–1433.

Nayak RK, Albert EN, Kassira WN, 1976b: Ultrastructural studies of prepubertal porcine uterine tube epithelium: Am J Vet Res **37**, 1001–1010.

Nayak RK, Zimmerman DR, Albert EN, 1976c: Electron microscopic studies of estrogen-induced ciliogenesis and secretion in uterine tube of the gilt: Am J Vet Res **37**, 189–197.

Nayak RK, Kassira WN, Albert EN, 1977: Light and electron microscopic studies of the porcine fetal uterine tube (oviduct): Am J Vet Res **37**, 1421–1433.

Odor DL, Blandau RJ, 1973: Egg transport over the fimbrial surface of the rabbit oviduct under experimental conditions: Fertil Steril **24**, 292–300.

Odor DL, Blandau RJ, 1985: Observations on the solitary cilium of rabbit oviductal epithelium: Its motility and ultrastructure: Am J Anat **174**, 37–453.

Odor DL, Gaddum-Rosse P, Rumery RE, Blandau RJ, 1980: Cyclic variations in the oviductal ciliated cells during the menstrual cycle and after estrogen treatment in the pig-tailed monkey, *Macaca nemestrina*: Anat Rec **198**, 35–57.

Pollard JW, Plante C, King WA, Hansen PJ, Betteridge KJ, Suarez SS, 1991: Fertilizing capacity of bovine sperm may be maintained by binding to oviductal epithelial cells: Biol Reprod **44**, 102–107.

Rumery RE, Gaddum-Rosse P, Blandau RJ, Odor DL, 1978: Cyclic changes in ciliation of the oviductal epithelium in the pig-tailed macaque (*Macaca nemestrina*): Am J Anat **153**, 345–366.

Smith TT, Koyanagi F, Yanagimachi R, 1987: Distribution and number of spermatozoa in the oviduct of the golden hamster after natural mating and artificial insemination: Biol Reprod **37**, 225–234.

Sorokin SP, 1968: Reconstructions of centriole formations and ciliogenesis in mammalian lungs: J Cell Sci **3**, 207–230.

Stalheim OHV, Gallagher JE, Deyoe BL, 1975: Scanning electron microscopy of the bovine, equine, porcine, and caprine uterine tube (oviduct): Am J Vet Res **36**, 1069–1075.

Steinman RM, 1968: An electron microscopic study of ciliogenesis in developing epidermis and trachea in the embryo of *Xenopus laevis*: Am J Anat **122**, 19–56.

Suarez S, Redfern K, Raynor P, Martin F, Phillips DM, 1991: Attachment of boar sperm to mucosal explants of oviduct *in vitro*: Possible role in formation of a sperm reservoir: Biol Reprod **44**, 998–1004.

Verhage HG, Brenner RM, 1975: Estradiol-induced differentiation of the oviductal epithelium in ovariectomized cats: Biol Reprod **13**, 104–111.

Verhage HG, Bareither ML, Jaffe RC, Akbar M, 1979: Cyclic changes in ciliation, secretion and cell height of the oviductal epithelium in women: Am J Anat **156**, 505–522.

Wu ASH, Carlson SD, First NL, 1976: Scanning electron microscopic study of the porcine oviduct and uterus: J Anim Sci **42**, 804–809.

Yaniz JL, Lopez-Gatius F, Hunter RHF, 2006: Scanning electron microscopic study of the functional anatomy of the porcine oviductal mucosa: Anat Histol Embryol **35**, 28–34.

Author's address (for correspondence): Hiroyuki Abe, Tohoku University Biomedical Engineering Research Organization, 6-6-07 Aoba, Aramaki, Aoba-ku, Sendai, Miyagi 980–8579, Japan. E-mail: abe@tubero.tohoku.ac.jp

—Mini Review—

Evaluating the Quality of Human Embryos with a Measurement of Oxygen Consumption by Scanning Electrochemical Microscopy

Takafumi Utsunomiya[1]*, Kaori Goto[1], Megumi Nasu[1], Yoko Kumasako[1], Yasuhisa Araki[2], Masaki Yokoo[3], Takahiro Itoh-Sasaki[4] and Hiroyuki Abe[4]

[1]St-Luke Clinic, 5 Tsumori Tomioka, Oita City, Oita 870-0947, Japan
[2]The Institute for ARMT, Gunma 371-0105, Japan
[3]Innovation of New Biomedical Engineering Center, Tohoku University, Sendai 980-8574, Japan
[4]Graduate Program of Human Sensing and Functional Sensor Engineering, Graduate School of Science and Engineering, Yamagata University, Yonezawa 992-8510, Japan

Abstract: Morphological evaluation has been widely used to evaluate embryo quality because it is non-invasive and useful in predicting pregnancy rate. However, morphological evaluations are subjective and categorization standards often vary between investigators. The respiration rate of embryos is a useful parameter for evaluating embryo quality. The scanning electrochemical microscopy (SECM) measuring system provides a non-invasive, simple, accurate, and consistent measurement of the respiration activity of human embryos. After morphological evaluation by Veeck's method, oxygen consumption by individual human embryos was quantified by SECM. Fundamentally, the maturation of mitochondria correlated with an increase in oxygen consumption during the development of embryos. The development of mitochondria may be an important factor in embryo quality, because mitochondria provide ATP for embryonic development by metabolism of nutrients in the cytoplasm. The respiration rates on the day 3 after in vitro fertilization (IVF) were measured and significant differences in oxygen consumption were registered even among embryos with the same morphological classification. There were no significant differences between the mean rates of oxygen consumption at each cleavage stage, however, there was considerable variation in respiration rate within embryos of the same morphological grade. The safety of SECM is assured as the embryos which were examined by SECM for oxygen consumption showed the same development levels as the control group. These results support the hypothesis that measuring embryonic respiration provides additional and valuable information about embryo quality.

Key words: Embryo quality, Oxygen consumption, Non-invasive evaluation

Introduction

Morphological evaluation has been widely used to evaluate embryo quality because it is non-invasive and useful in predicting pregnancy rates. However, morphological evaluations are subjective and categorization standards often vary among investigators. Therefore, more objective selection criteria are needed. Respiration is a useful parameter for evaluating embryo quality as it provides important information about metabolic activity. The scanning electrochemical microscopy (SECM) measuring system, which was introduced by Abe et al. [1], provides a non-invasive, simple, accurate, and consistent measurement of the respiration activity of single human embryos.

Scanning electrochemical microscopy is a technique in which the tip of a microelectrode is used to monitor the local distribution of electro-active species near the sample surface. The SECM measuring system has
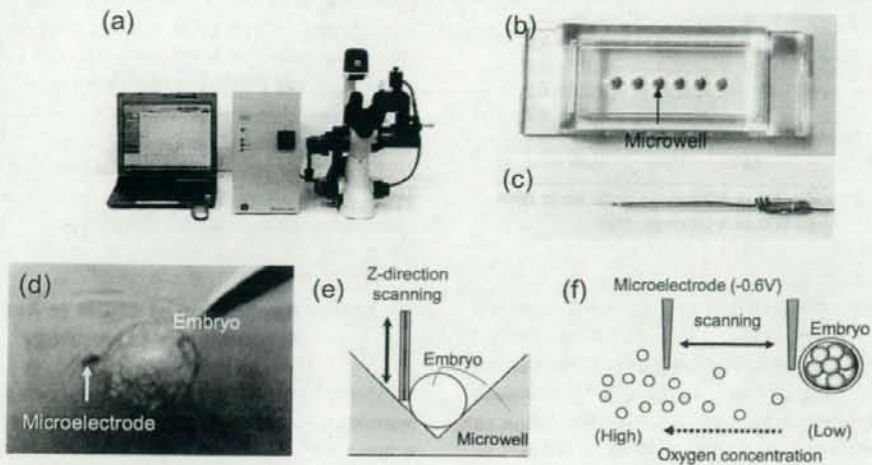
SECM system

Fig. 1. The SECM system (a), a plate with microwells (b), and a microelectrode (c) for measurement of respiration activity of embryos. SECM includes a measurement instrument on the inverted optical microscope stage, a potentiostat, and notebook computer. The plate has six cone-shaped microwells (arrow). Individual embryos are transferred into a microwell filled with HFF99 medium. The sample sinks to the bottom of the well remaining at the lowest point (d, e). The oxygen concentration profiles are calculated with custom software based on spherical diffusion theory (f). Measurements of each embryo are performed very rapidly.

been used to non-invasively measure respiration activity of single bovine and murine embryos, among other species [2]. We employed SECM to accurately determine the oxygen consumption of single, identical human embryos at different developmental stages. In this article, we introduce the SECM method for assessing the quality of individual human embryos.

Measuring Respiration Activity of Single Human Embryo

Following *in vitro* fertilization (IVF)-embryo transfer procedure, surplus embryos that patients preferred not to keep preserved were used in our study. Informed consent for use of the embryos in this research was obtained from all the patients. From July 2006 to July 2007, 188 embryos from 73 cycles were examined. The mean age of the embryo donor was 34.5 ± 4.5 years and the number of previous ART cycles was 2.7 ± 2.3.

The embryos were cultured in Cleavage Medium (Sydney IVF, Australia) until day 3, after which they were cultured in Blastocyst Medium (Sydney IVF,

Australia). After morphological evaluation by Veeck's method, oxygen consumption of individual human embryos was quantified with a modified SECM measuring system (Fig. 1). A single embryo was transferred into a well filled with HFF99 (Fuso Pharmaceutical Industries, Osaka, Japan) medium, where it fell to the bottom of the cone-shaped microwell and remained at the lowest point. A platinum (Pt)-microdisk electrode was lowered into the solution, and its tip potential was held at −0.6V vs Ag/AgCl with a potentiostat to monitor the local oxygen concentration. The microelectrode scanned along the z-axis from the edge of the sample and the oxygen consumption rate was calculated with custom software based on spherical diffusion theory. Measurements of each embryo were performed very rapidly (within 1 min). A part of each embryo was prepared for observation by transmission electron microscopy. The safety of SECM on the embryos was also examined.

The mean respiration rates ($F \times 10^{14}$/mol·s^{-1}) of 4-cell, 5-cell, 6-cell, 7-cell, 8-cell, 9-cell, and 10-cell embryos were 0.34 ± 0.1 (n=8), 0.45 ± 0.2 (n=15), 0.37 ± 0.1

Table 1. Oxygen consumption rates at each cleavage stage

Cleavage stage	No. of embryos examined	Oxygen consumption $(F \times 10^{14}/\text{mol·s}^{-1})$
4-cell	8	0.34 ± 0.1
5-cell	15	0.45 ± 0.2
6-cell	39	0.37 ± 0.1
7-cell	51	0.39 ± 0.2
8-cell	50	0.40 ± 0.2
9-cell	12	0.40 ± 0.1
10-cell	12	0.50 ± 0.2

There were no significant differences in the mean rates of oxygen consumption at each cleavage stage.

(n=39), 0.39 ± 0.2 (n=51), 0.40 ± 0.2 (n=50), 0.41 ± 0.1 (n=12), and 0.50 ± 0.2 (n=12), respectively (Table 1). There were no significant differences between the mean respiration rates at each cleavage stage; however, there was considerable variation in respiration rate within embryos of the same morphological grade.

The relationship between the embryo morphology and oxygen consumption was examined (Fig. 2). Significantly different levels of oxygen consumption were registered even among embryos of the same morphological classification.

After measuring their respiration rates with SECM, embryos were cultured to examine their developmental capacity. Embryos with moderate respiration rates (more than 0.26×10^{14} /mol·s^{-1} and under 0.56×10^{14}/ mol·s^{-1}) had a 65.8% chance of reaching the blastocyst stage. On the other hand, embryos with lower (under 0.25×10^{14}/mol·s^{-1}) and higher (more than 0.55×10^{14} mol·s^{-1}) respiration rates had only a 39.0% chance of reaching the blastocyst stage (Fig. 3).

The safety of SECM is assured as the embryos which were examined by SECM for oxygen consumption showed the same levels of development as the control group (Fig. 4).

Future Application of SECM in Assisted Reproductive Technology

Finding embryos of the highest quality is an imperative for obtaining good results in ART. To obtain a good embryo, many reports have proposed new methods and findings. A report on the correlation between first polar body morphology and pregnancy rate suggested that preselection at a very early stage may be helpful in identifying a subgroup of preimplantation embryos with good prognosis to form

Individual human embryos on DAY3 after IVF and oxygen consumption rate.

	I	II	III	IV	V	VI
Morphology of embryos						
Classification by Veeck method	4-cell Grade 1	4-cell Grade 1	6-cell Grade 2	6-cell Grade 2	8-cell Grade 2	8-cell Grade 2
Oxygen consumption $(F \times 10^{14}/\text{mol·s}^{-1})$	0.25	0.44	0.57	0.23	0.71	0.35

Fig. 2. Individual human embryos on Day 3 after IVF were classified by the method of Veeck *et al*. There were considerable variations in respiration rates within embryos (I and II, III and IV, V and VI) classified as the same morphological grade.